

Validation of the Ballistic Limit Equation for Monolithic Aluminum Shielding at Geostationary
Orbital Debris Impact Velocity

A Senior Project
presented to
the Faculty of the Aerospace Engineering Department
California Polytechnic State University, San Luis Obispo

In Partial Fulfillment
of the Requirements for the Degree
Bachelor of Science

by

Brandon Holladay

October, 2012

© 2012 Brandon Holladay

Validation of the Ballistic Limit Equation for Monolithic Aluminum Shielding at Geostationary Orbital Debris Impact Velocity

Brandon Holladay¹

California Polytechnic State University, San Luis Obispo, CA 93401

The Cal Poly Electro Magnetic Rail Gun was used to eject a 0.370 gram, rectangular aluminum projectile towards a 1/16 inch monolithic aluminum plate at a speed of 280 ± 50 m/s. The resulting impact left a large attached spall on the back of the shielding. The impact damage was compared to an industry ballistic limit equation for a spherical aluminum projectile of similar diameter and was shown to have slightly less damage than the expected results.

In addition, an aluminum mesh double bumper shield was fired upon in order to verify its higher protection per aerial density as well as its higher projectile break-up ability. An impact at 459 ± 50 m/s resulted in superior shielding performance over an aluminum monolithic shield of equivalent areal density, based on the ballistic limit equation; however projectile break up did not occur. A minimum mass savings of 23% was realized using the mesh double bumper shield. Furthermore, when an additional aluminum bumper was placed in front of the mesh bumper, even greater ballistic protection was achieved with a minimum mass savings of over 65%.

Nomenclature

BHN	=	Brinell hardness number
C_t	=	speed of sound in shielding material
d_c	=	critical projectile diameter
FPS	=	frames per second
k	=	damage parameter
t	=	shield thickness
V	=	projectile velocity
Θ	=	angle of impact
ρ_t	=	density of shielding material
ρ_p	=	density of projectile material

I. Introduction

Micro meteorite and orbital debris pose a significant danger to orbiting spacecraft. As the number of spacecraft in orbit continues to grow each year, the debris associated with the launch and operation of spacecraft, continues to grow as well. Additional debris is also created from the

¹ Student, Aerospace Engineering, 1 Grande Avenue, San Luis Obispo, CA 93401.

impact of existing space objects with other spacecraft, spent rocket bodies, etc. As the threat from orbital debris increases, so must the measures taken to protect costly spacecraft from catastrophic impact.

At geostationary altitudes, only objects that are greater than roughly 1 meter can be detected and tracked from Earth due to limitations on observing instruments¹. As a result, active MMOD protective techniques, such as maneuvering space vehicles out of the path of incoming debris, are not feasible for protection against objects smaller than 1 meter. Instead, more passive techniques must be implemented, such as placing vital payload components away from areas expected to see the highest debris flux, designing with redundancies, or shielding by either bulking up existing spacecraft structural material or directly through specifically designed ballistic shields¹.

A. Overview of the GEO debris environment

While exact debris flux numbers for geostationary orbits are hard to find and at best are very rough estimates, it is thought that the average flux is approximately 1/100th that which is found in low earth orbit (LEO)¹. Figure 1 is a representation of the approximate flux in and around GEO. At GEO altitude, the estimate flux is on the order of 10^{-8} object per square meter per year. Although a comparatively small flux to that of LEO, this had lead to an expected explosion rate per GEO satellite of 4×10^{-4} per year based on known collisions and the number of cataloged objects at GEO². At this rate, the amount of orbital debris at GEO is expected to grow significantly in the years to come, as can be seen in Fig. 2, making the risk of collision a more crucial factor in spacecraft design.

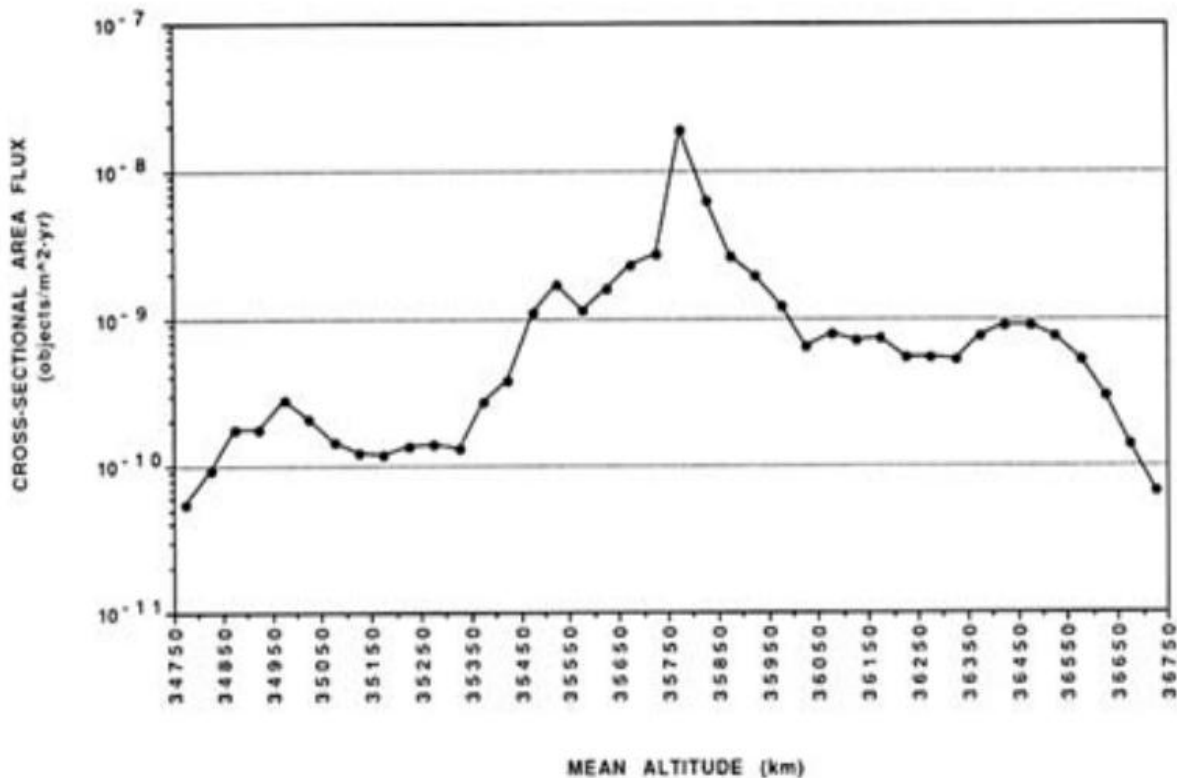


Figure 1. MMOD cross-sectional flux estimate at GEO altitudes as of 1995¹.

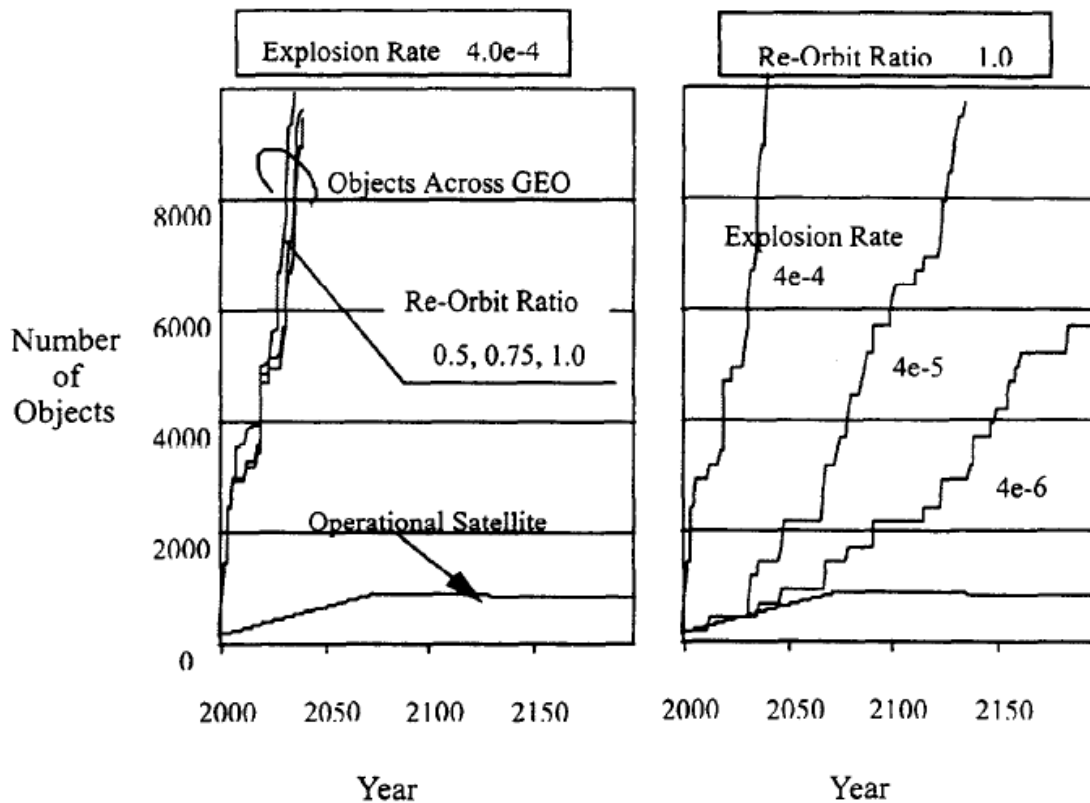


Figure 2. Estimated increase in objects at Geosynchronous altitudes².

Orbital velocity at GEO is 3.07 km/s. As a result, a head on collision will see impact velocities of about 6 km/s. However, due to the nature of the orbit, most spacecraft, as well as most orbital debris, travel in the same direction making head on collisions exceedingly rare even by space impact terms¹. In addition, due to the natural inclination drift of uncontrolled objects in GEO, the majority of impacts from orbital debris will come from objects in inclined or eccentric orbits¹. Consequently, the average impact speed seen from orbital debris at GEO is roughly 500 m/s¹. This is relatively low in terms of on orbit impact speeds, well below the hypervelocity impacts associated with LEO objects. However, impacts in excess of 500 m/s can still cause catastrophic damage to unshielded spacecraft.

Due to the expected growth of space debris in the GEO regime, it is important that more impact testing of ballistic shielding at these speeds be conducted in order to develop lightweight, low volume, and low cost shielding suitable for GEO spacecraft.

B. Overview of the Cal Poly Electro Magnetic Rail Gun

In 2011, four Cal Poly Aerospace engineering undergraduates led by Jeffrey Maniglia, designed, fabricated, and successfully tested an Electro Magnetic Rail gun, or EMRG. The Mach 1, as it has come to be called, utilizes a capacitor bank to store energy and to quickly discharge the large electric potential through the conductive projectile³. Through a phenomenon known as the Lorentz Force, which occurs in the presence of a magnetic field and an electric current, the projectile is propelled along the conducting rails. The velocity at which the

projectile can be propelled is heavily dependent on the amount of electrical energy being discharged across the rails and as such, the maximum velocity of an EMRG is only limited by the energy storage and discharge system, as well as material limitations. This is an advantage over traditionally used light-gas guns since the acceleration of projectiles fired by these systems are limited by the expansion rate of the gas used³.

The first full power, successful test, fired an aluminum projectile at over 650 m/s. Subsequent tests of the Mach 1 have fired between 280 and 459 m/s. It was determined that a new power system, as well as changes to the rail system, would be needed in order to fire at higher velocities and with greater frequency. However, while the new power and rail systems were being developed, it was convenient to utilize the Mach 1 for experimentally simulating GEO debris impacts.

C. Orbital Debris Shielding

Generally speaking, spacecraft debris shielding falls into two main categories: monolithic and Whipple shielding.

Monolithic shielding refers to a single wall or plate used to protect against incoming debris. Plate materials can range from metallics such as aluminum or titanium, to composite reinforced materials, and to even the glass and polycarbonate materials used to protect spacecraft windows. Monolithic shields generally require more mass than Whipple shields however, they do not take up as much volume and are relatively uncomplicated while being cheap and easy to manufacture. Monolithic shields perform best at low impact velocities below 2 to 3 km/s.

At higher velocities, the enormous amount of energy from the impact is enough to break up or even vaporize the particle and shielding materials. This is beneficial because after the initial impact, the particle debris is spread over a larger area, making it easier to shield. Whipple shields take advantage of this higher velocity impact characteristic by utilizing multiple plates or bumpers to first break up the particle and then shield against the resulting debris clouds and shockwaves from the impact. Using this method, a Whipple shield is able to protect against more massive and higher velocity orbital debris, then a monolithic shield with equivalent mass, as illustrated in Fig. 3. The point at which the Whipple shield is able to start breaking up

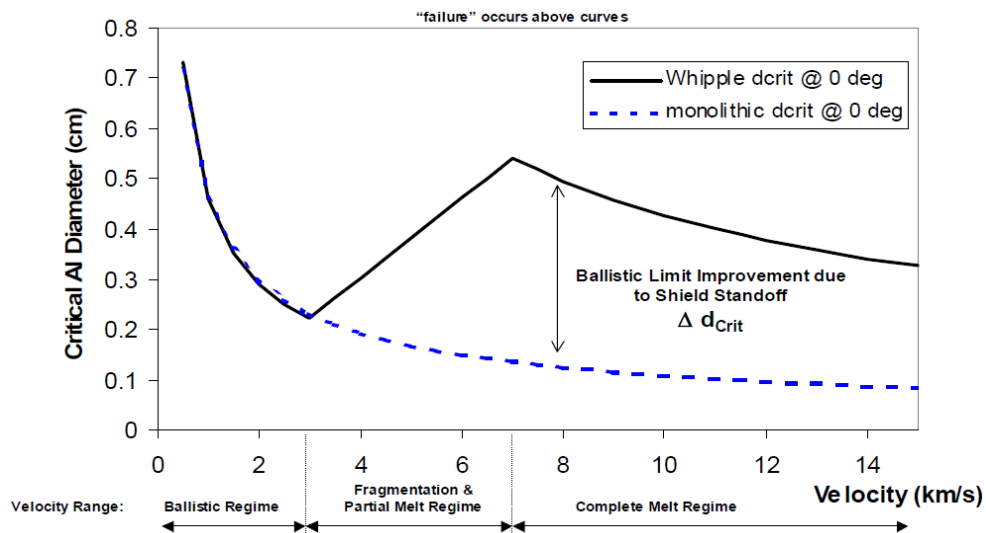


Figure 3. Failure curves for Al on Al monolithic and Whipple shielding⁴.

impacting particles is when it begins to outperform monolithic shielding. The major drawback of Whipple shielding is the volume it requires. With standoff distances between the front and rear bumpers being anywhere from 10 to 30 cm or more, launch vehicle requirements may become an issue. However, with recent advances in flexible and deployable shields, it is likely that this will become less of an issue in the future⁵.

Despite advances in Whipple shield technology, it is still necessary to test and develop monolithic shielding. Specific areas on spacecraft where Whipple shield placement is impractical or inconvenient, monolithic shielding will be necessary.

II. Objective

The goals of this project are three fold. First, this project will provide ballistic shielding for the Cal Poly Electromagnetic Rail Gun team to utilize for test firings. Various ballistic shields were created for this purpose. The second and main objective was to experimentally test the monolithic ballistic limit equation for aluminum at average geostationary orbit impact speeds. Lastly, this project will provide the groundwork for developing more advanced ballistic shielding as the projectile velocity capabilities of the EMRG improve.

III. Apparatus

The EMRG system consists of two 36 inch long copper rails spaced 0.25 inches apart and supported by Garolite-11, Teflon, and Fiberglass as seen in Fig 4. A 10,000 μ F capacitor bank system is used to supply a charge of over 450 volts across the rails³.

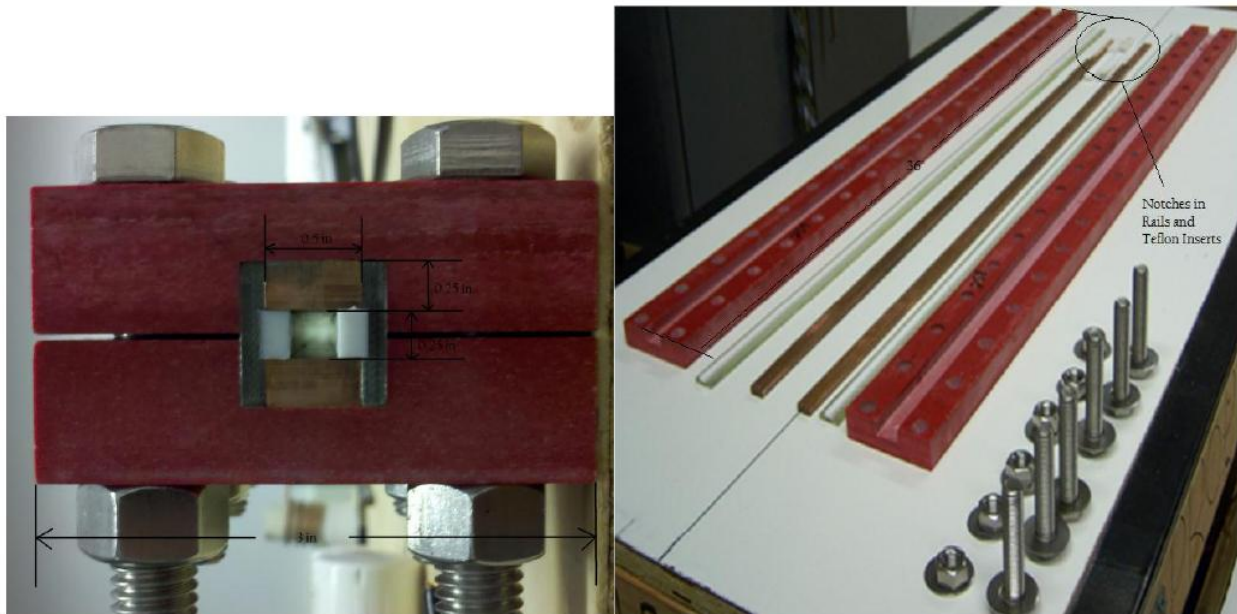


Figure 4. Inner Dimensions (left) and length (right) of finished prototype rails.³

A high speed camera capable of taking 15,000 frames per second is positioned normal to the path of the projectile and protected inside a wood and Plexiglas container. After testing of the monolithic shielding, the camera was then upgraded for all later testing to one capable of 62,000 frames per second. A whiteboard was positioned parallel to the path of the projectile with grid squares of dimension 2 x 2 inch, as seen in Fig. 5.

The catching mechanism consists of a wooden box located approximately one meter from the rail gun system. The ballistic shield was originally attached inside the box, but with the addition of the high speed camera, the box was moved to the outside in order to provide a more clear view of the projectile impact on the shield. Within the box and behind the shielding is approximately 25 cm of hardened foam insulation, followed by a three quarter inch steel plate.

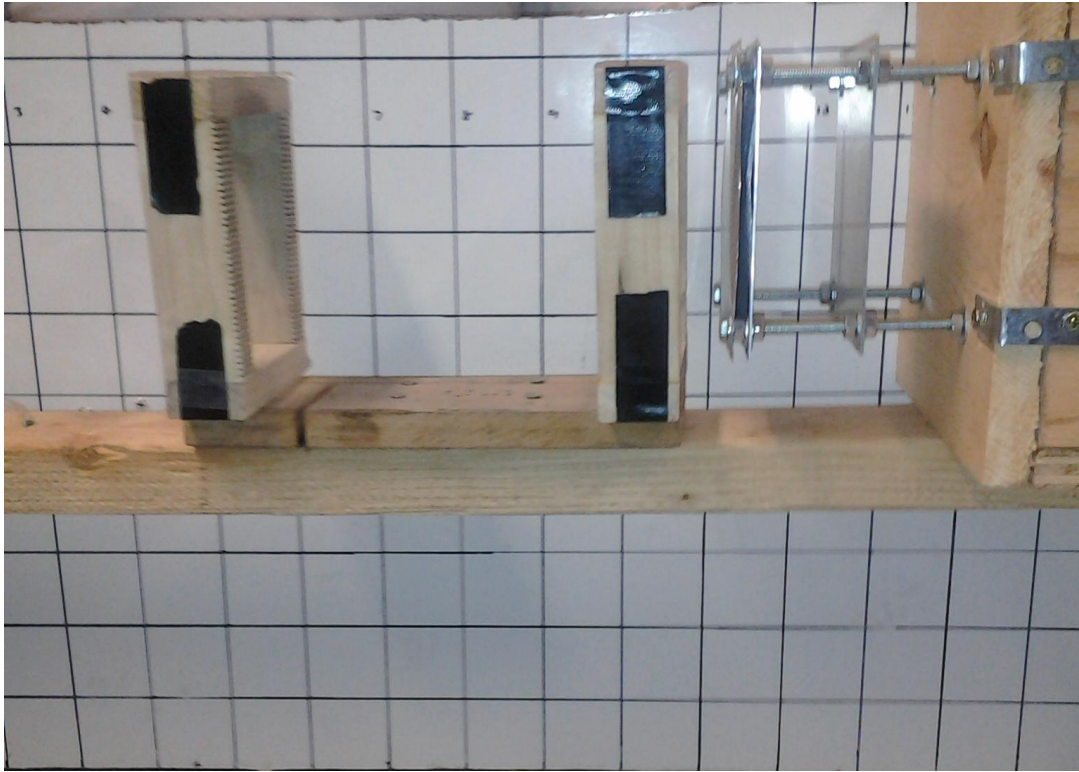
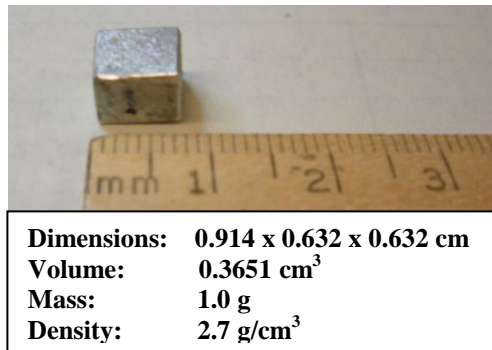


Figure 5. Projectile shield and whiteboard grid apparatus.

The projectile, seen in Fig. 6, is a rectangular aluminum cube of dimensions 0.249 x 0.249 x 0.36 inch with a mass of approximately one gram. It is important to note that some of the mass of the projectile is lost inside the rail system due to melting. Recent improvements in decreasing the amount of arcing and plasma within the rail system will hopefully significantly decrease the projectile mass loss.



Dimensions:	0.914 x 0.632 x 0.632 cm
Volume:	0.3651 cm³
Mass:	1.0 g
Density:	2.7 g/cm³

Figure 6. Aluminum projectile before EMRG firing.

IV. Ballistic Limit Equations

A ballistic limit equation (BLE) is used to determine how much damage a ballistic shield will sustain from a high velocity impact. Most BLE's are created from empirical impact data and as a result, are subject to change when more data is available. Ballistic limit equations are an essential tool for determining the minimum shielding requirements for spacecraft.

The ballistic limit equation for an aluminum monolithic shield is given by⁷,

$$d_c = \left[\frac{t \text{ BHN}^{0.25} (\rho_t / \rho_p)^{0.5}}{k 5.24 (V \cos \theta / C_t)^{2/3}} \right]^{18/19}$$

where d_c is the critical projectile diameter in cm for the given damage parameter, k is the damage parameter, BHN is the Brinell hardness of the target, C_t is the speed of sound of aluminum in km/s, V is the projectile speed in km/s, θ is the angle normal to impact in degrees, and ρ_t and ρ_p are the densities of the target and projectile respectively.

Using an iterative method and given the projectile diameter and velocity, the expected damage parameter can then be solved. For an aluminum monolithic shield, a damage parameter of greater than 3 results in cratering upon the front of the plate but no spalling behind the plate, between 2.2 and 3 results in an attached spall and 1.8 to 2.2 is a detached spall, while anything less than 1.8 is a complete perforation of the plate. It should be noted that this damage parameter is not comparable with other types of shielding.

While this BLE is designed for a spherical projectile and not a rectangular projectile, impact damage for aluminum projectile diameters below 0.92 cm is more dependent upon the diameter of the projectile than it is upon the mass (See Appendix A). As such, it is expected that the rectangular projectile hitting the plate in the plane of its smallest dimensions would be comparable to that of a sphere with a similar diameter. However, due to the higher mass of the rectangular projectile, a slightly more severe damage parameter would be likely. On the other hand, should the projectile impact on the plane of its largest dimensions, the mass of the projectile would play a larger role and the damage of the projectile would be more comparable to a sphere with a similar mass.

V. Projectile Velocity

Determining the projectile velocity at the time of impact is critical to analyzing the accuracy of the BLE as well as determining the capability of the EMRG. For this purpose, the high speed camera and whiteboard grid were utilized. By counting the number of frames the projectile takes to travel across the 2 inch grid and knowing the frames per second of the video, a determination of velocity can be calculated.

$$\text{Velocity} = \frac{\text{Distance}}{(\text{frames}/\text{FPS})}$$

where FPS is the frames per second of the high speed video. Due to deceleration, it is important that the velocity be calculated when the projectile is as close to the ballistic shield as possible. However, with the large amount of super heated gas obscuring the visibility of the projectile

when close to the shield, this can be difficult. One method proposed to correct for this is to determine the velocity and rate of deceleration of the projectile when it is last visible and estimate the speed of impact, given the remaining distance that the projectile must travel. However, for many impacts, the projectile was not visible for a sufficient amount of time to determine deceleration. For these impacts, the last known velocity was used.

VI. Monolithic Shield Test Results

A 1/16 inch thick aluminum monolithic shield was impacted by an aluminum projectile at a rate of 280 ± 50 m/s, based on high speed video footage. Figure 7 is a still frame of the EMRG firing. As can be seen, a large super heated gas cloud is ejected from the rail gun. This made determining the velocity of the projectile very difficult since the gas cloud obscured the projectile during many of the frames. In addition, from the high speed video footage, very small metallic fragments can be seen being ejected from the EMRG including one larger fragment that was mistaken for the projectile. These fragments are likely pieces from the original projectile that broke off or melted within the rails of the EMRG. Slight damage from these small fragments can be seen on the plate, although it is negligible.

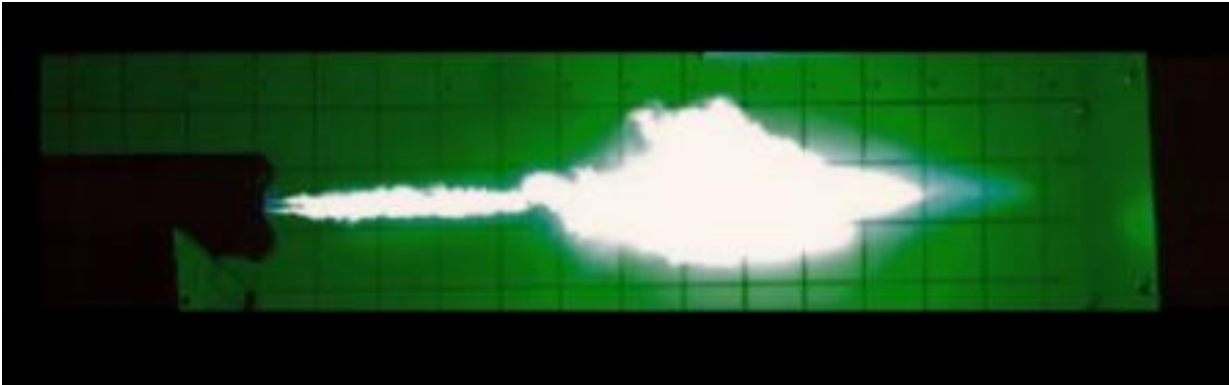


Figure 7. Still frame of EMRG firing on aluminum monolithic shield.

The impact of the projectile left a crater with a diameter of approximately 2.5 cm across, seen in Fig 8. The resulting spall from the crater was left completely intact, although the plate appeared to be close to its maximum amount of spalling before detachment occurs. The damage observed lead to a damage parameter of 2.2 to 2.4 to be determined for the plate.



Figure 8. Front (left) and back (right) aluminum monolithic plate damage.

Based on plate and projectile damage, the projectile appears to have impacted slightly off plane (about 15 to 20 degrees) of the projectile's smallest dimensions and did not appear to break apart. In addition, the projectile appears to have suffered some additional impact damage due to a ricochet, although this is uncertain. As can be seen from Fig. 9, the projectile density significantly decreased. This is likely due to the large amounts of electric current that went through the projectile while inside the rails.

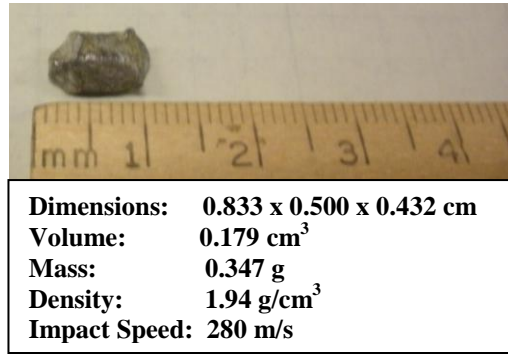


Figure 9. Projectile after impact with aluminum monolithic plate.

For the purposes of comparing the impact damage to that from the BLE, the average diameter of 0.46 cm was used. At a velocity of 280 m/s a damage parameter of 2.05, or a detached spall, would be expected.

Based on this impact, the ballistic limit equation for the aluminum monolithic shield would appear to provide a conservative answer for the necessary shielding thickness required for a 0.347 gram rectangular aluminum projectile impacting head on at around 280 m/s. However, much more data is needed, including oblique impacts and impacts in which the projectile hits the plate along its large side.

The remodeling of the rail gun, which is occurring at the time of this writing, will allow for additional impact testing upon monolithic shields and more extensive data.

VII. Other Ballistic Shield Test Results

A. Aluminum Mesh Double Bumper Shield

Projectile break up is essential to greatly increasing the effectiveness of a bumper shield. However, at velocities less than 1 to 2 km/s, projectiles often remain intact after initial impact. One method used to increase the chance of break up is to simply increase the shielding thickness of the first bumper. This can be costly in terms of mass and so other methods which keep additional mass to a minimum, have been researched. One such method is to use a sacrificial aluminum mesh in front of the first bumper⁶. The aluminum mesh is able to provide the break up potential of a thicker bumper and equivalent stopping power, with a fraction of the mass cost. Two such shields were created for testing with the EMRG.

The first, seen in Fig. 10, is comprised of 50 by 50, 0.23 diameter aluminum mesh, followed by a 1/32 inch aluminum plate. A 1/16 inch aluminum plate is placed at a standoff of 2 inches. The EMRG fired the projectile at a speed of 459 ± 50 m/s, perforating both the mesh and 1/16 inch bumpers and leaving an attached spall on the 1/16 inch back bumper. The damage upon the back plate was estimated to be the equivalent of 2.8 for an aluminum monolithic shield. The projectile impacted along the plane of its smallest dimensions and was left intact.

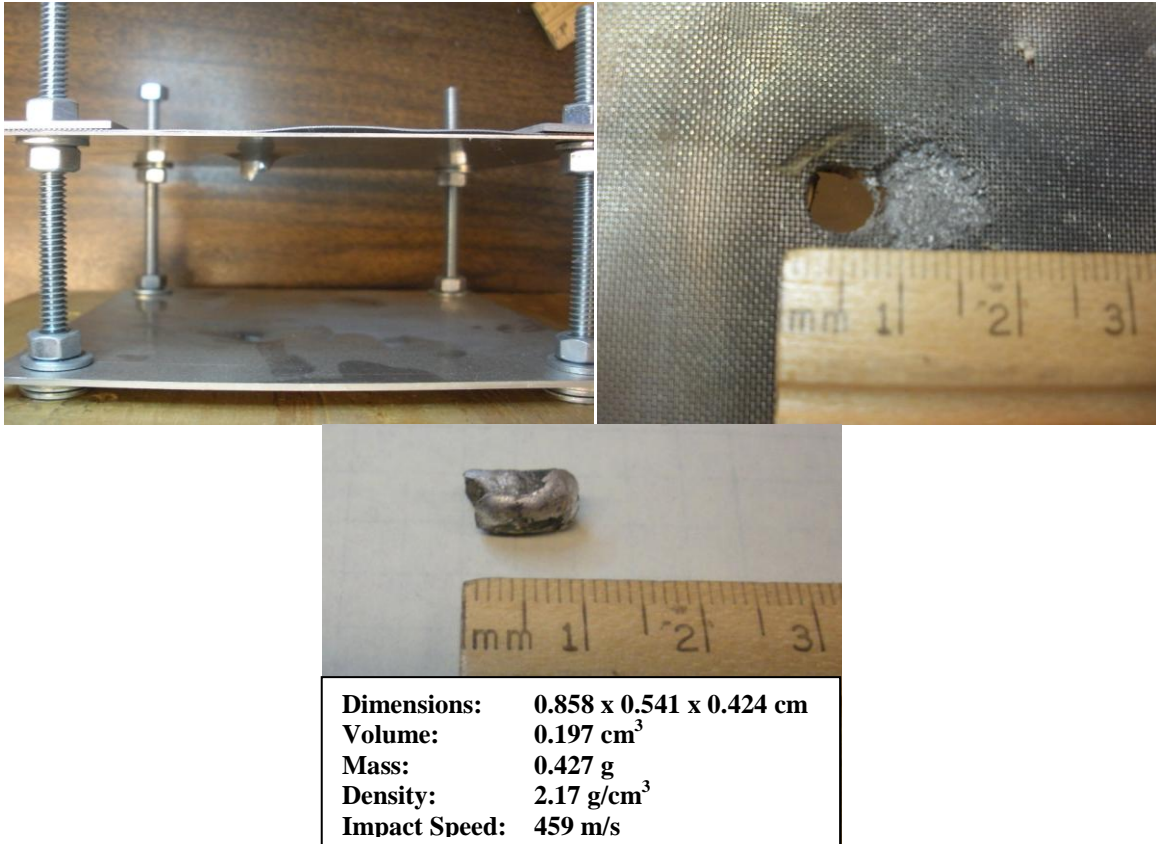


Figure 10. Impact damage on mesh double bumper (top) and projectile (bottom).

With a total areal density of 7.137 kg/m^2 for the bumpers with which the projectile contacted, the mesh shield can be compared to a monolithic aluminum shield of 0.255 cm or approximately 1/10 inch thick, which has the same areal density as the mesh shield. Based on the aluminum monolithic BLE, a projectile of similar properties and impacting at the same velocity would be expected to have a damage parameter of between 2.15 and 1.9, or a detached spall from the plate. Additionally, the damage upon the back plate of the mesh shield was estimated to be the equivalent of 2.8 for an aluminum monolithic shield. A minimum areal density of about 9.243 kg/m^2 would be necessary to see an equivalent amount of shielding protection – a mass savings of about 23%.

It was thought that due to the low velocities, the temperature of the projectile was not high enough at the time of impact to initiate break up. A second mesh shield was built that incorporated a 1/128 inch aluminum plate placed 3/8 inch in front in order to increase the thermal state of the projectile before impact with the mesh bumper.

The EMRG fired the projectile at 449 m/s and the resulting damage can be seen in Fig.11. The projectile impacted along the plane of its smallest dimensions, completely perforating the 1/128 inch plate and leaving a sizable attached spall on the 1/32 inch plate. The projectile did not appear to have broken up at all.

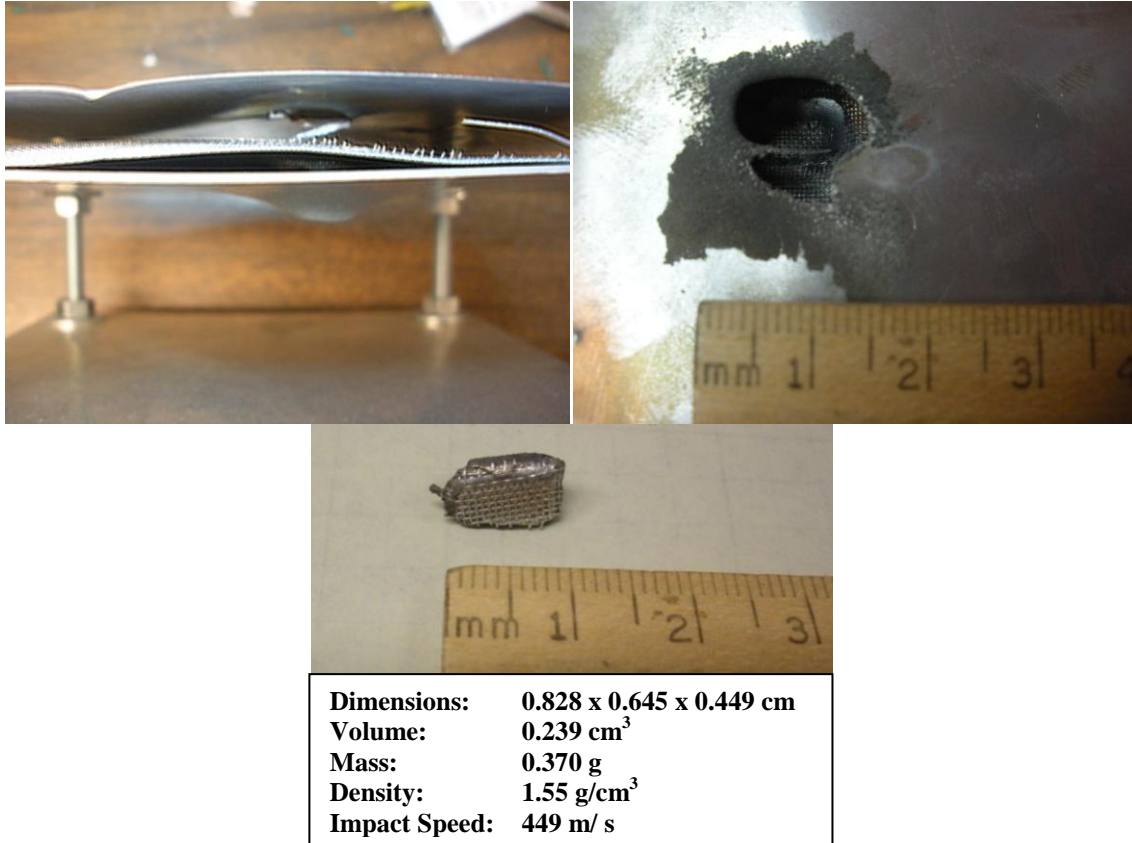


Figure 11. Impact damage on mesh double bumper shield with additional front plate (top) and projectile damage (bottom).

The areal density of the bumpers with which the projectile came into contact totaled 3.248 kg/m². This is equivalent to a monolithic aluminum bumper of approximately 0.116 cm or a little less than 1/20 inch thick. A projectile of similar properties and impacting at the same velocity would be expected to produce a damage parameter of 0.75 to 0.72, easily perforating the plate. The damage upon the bumper appeared to be at the spalling limit, or the equivalent of about 2.2 to 2.3 for an aluminum monolithic shield, which would require a monolithic shield with a minimum areal density of 9.451 kg/m² based on the BLE – a mass savings of over 65%.

While the density of the projectile was significantly less and the impact was on a different side making a performance comparison of the two mesh shields difficult, it would seem that the additional front bumper significantly increased the protective potential of the mesh shield. However, additional testing of monolithic shields with comparable areal densities, as well as additional testing on mesh shields, must be done in order to validate these results.

B. Aluminum Multiple Bumper

A multiple bumper shield, comprised of 6, 1/128 inch aluminum bumpers followed by one 1/16 inch aluminum back bumper, was constructed in order to display the progression of the projectile through multiple bumpers using the high speed video equipment. With the bumpers placed 3/8 inch apart, as seen in Fig. 12, the aluminum projectile perforated all the bumpers except the last, leaving only a very small spall. The velocity of the projectile could not be verified for this firing. The projectile remained intact following impact of the shield.

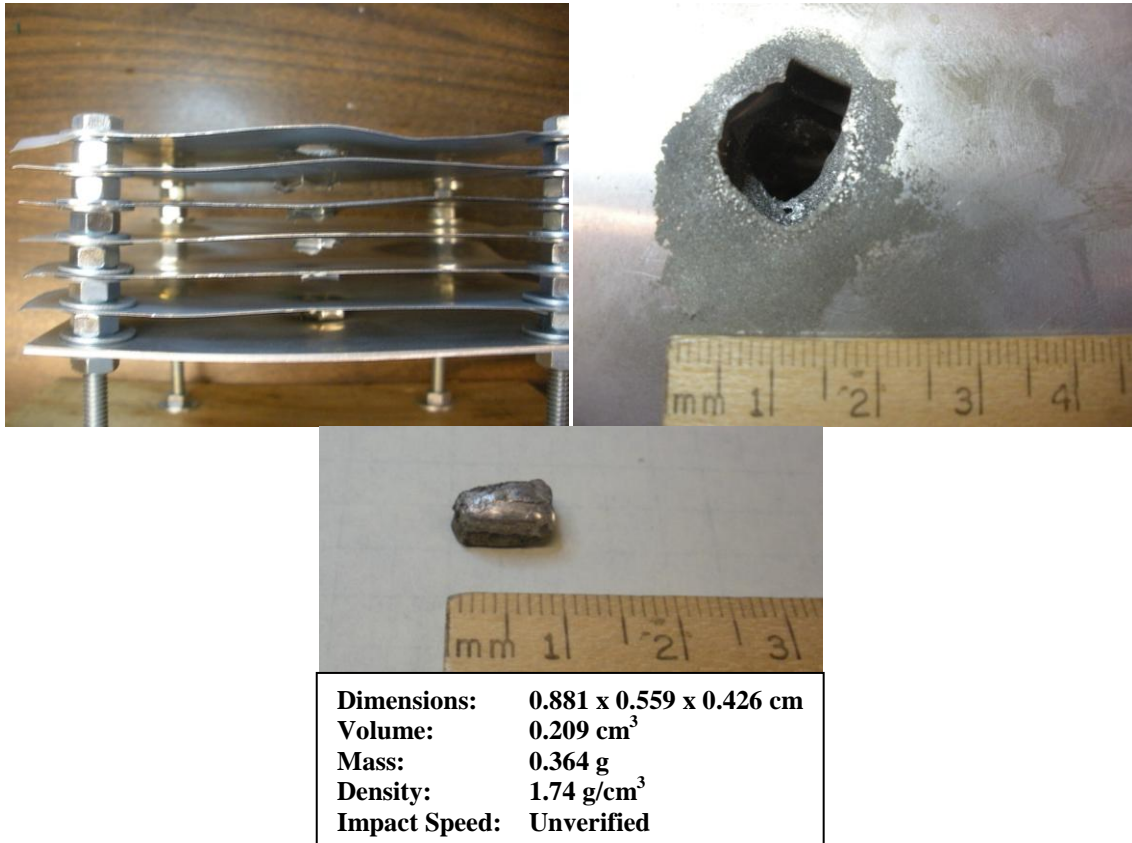


Figure 12. Impact damage on aluminum multiple bumper shield (top) and projectile damage (bottom).

VIII. Future Work

As the capabilities of the Cal Poly EMRG continue to increase, development and testing of more complex shielding for higher velocity projectiles can be done. Lightweight composite materials have shown to be extremely advantageous in stuffed Whipple shield designs and their continued development is very promising⁴.

There is also a need for progress to be made in projectile break-up capabilities at velocities below 3 km/s. Further investigation into mesh shielding as well as ultra high yield strength ceramic sacrificial layers is of great interest.

Lastly, impact testing of specific spacecraft structural and miscellaneous parts will also be of interest. This includes materials such as honeycomb paneling and carbon composites that are being utilized more and more as that technology develops.

IX. Conclusion

Comparison of experimental impact results and the ballistic limit equation for an aluminum monolithic shield showed the BLE to be slightly conservative. However based on the error associated with determining the velocity of the projectile at impact, the BLE results are still within the range of expected damage. Further impact testing upon monolithic shielding must be done in order to confirm the conservative results. In addition, steps have been taken in order to decrease the error associated with the projectile velocity such as using a camera capable of a higher frames per second rate and adding speed gates along the projectile path.

It was also found that adding an additional thin front bumper to a mesh bumper shield significantly improved the shield effectiveness and mass savings. Further mesh bumper shield testing should be conducted in order to determine if other bumper materials or combinations of, can further increase protection per areal density.

References

¹*Orbital debris: a technical assessment*. Washington, D.C.: National Academy Press, 1995. Print.

²Yasaka, T. Yasaka. "Geo Debris Environment: A Model to Forecast the Next 100years." *Advances in Space Research* 23.1 (1999): 191-99. *Science Direct*. Web.

³Maniglia, J., Smiroldo, J., Zohar, G., and Westfall, A.,. "Design, Fabrication, and Testing of an Electromagnetic Rail Gun for the Repeated Testing and Simulation of Orbital Gun Impacts ." *Cal Poly Digital Commons* (2011)

⁴ *Handbook for Limiting Orbital Debris*, NASA Handbook 8719.14, approved July 30, 2008.

⁵ Christiansen, E, JH Kerr, HM de la Fuente, and WC Schneider. "Flexible and deployable meteoroid/debris shielding for spacecraft." *International Journal of Impact Engineering* 23.1 (1999): 125-136. Print.

⁶ Christiansen, Eric L.. *Meteoroid/debris shielding*. Houston, TX: National Aeronautics and Space Administration, Lyndon B. Johnson Space Center, 2003. Print.

⁷Christiansen, E. L. (2009) NASA/TM-2009021478 *Handbook for Designing MMOD Protection*, NASA Johnson Space Center, Houston, TX.

Appendix A

Determination of the effect of mass of the projectile on damage parameter:

$$d_c = \left[\frac{t \text{ BHN}^{0.25} (\rho_t / \rho_P)^{0.5}}{k 5.24 (V \cos \theta / C_t)^{2/3}} \right]^{18/19}$$

$$k = \frac{t \text{ BHN}^{0.25} (\rho_t / \rho_P)^{0.5}}{d_c^{19/18} 5.24 (V \cos \theta / C_t)^{2/3}}$$

$$k = \frac{\left(\frac{4\pi i}{3}\right)t \text{ BHN}^{0.25} \rho_t^{0.5}}{(2r)^{19/18} \left(\frac{4\pi i}{3}\right) \rho_P^{0.5} 5.24 (V \cos \theta / C_t)^{2/3}}$$

$$k = \frac{\left(\frac{4\pi i}{3}\right)t \text{ BHN}^{0.25} \rho_t^{0.5}}{(2r)^{-35/18} \left(\frac{4\pi i}{3}\right) 2r^3 \rho_P^{0.5} 5.24 (V \cos \theta / C_t)^{2/3}}$$

$$k = \frac{\left(\frac{4\pi i}{3}\right)t \text{ BHN}^{0.25} \rho_t^{0.5}}{(2r)^{-35/18} \left(\frac{4\pi i}{3}\right) 2r^3 (\rho_P) \rho_P^{-0.5} 5.24 (V \cos \theta / C_t)^{2/3}}$$

$$k = \frac{\left(\frac{4\pi i}{3}\right)t \text{ BHN}^{0.25} \rho_t^{0.5}}{(2r)^{-35/18} 2(\text{Volume})(\text{Density}) \rho_P^{-0.5} 5.24 (V \cos \theta / C_t)^{2/3}}$$

$$k = \frac{\left(\frac{4\pi i}{3}\right)t \text{ BHN}^{0.25} \rho_t^{0.5}}{(2\text{radius})^{-35/18} 2(\text{Mass})(\rho_P^{-0.5}) 5.24 (V \cos \theta / C_t)^{2/3}}$$

EMRG Test Objectives and Results

Date of Firing: ____ / ____ / ____

Operators Present: Sign and print for all that apply. Note that at least two operators must be present for any firing. For definitions of the responsibilities of the operations consult "Responsibilities of Rail Gun Team".

	<i>Print</i>	<i>Sign</i>
Firing Director:	_____	_____
Safety Officer:	_____	_____
Data Recorder:	_____	_____
Operations Overseer:	_____	_____

Purpose of Test: Fill out for all parts that apply as instructed by the Firing Director.

Velocity Test: Planned velocity: _____ Actual velocity measured at: _____

Camera FPS: _____

Shielding Test: Shield material(s): _____

Thickness of shielding: _____

Layers/spacing of Shielding: _____

Expected result: _____

Experimental result: _____

